



How Likely Are Snowball Episodes Near the Inner Edge of the Habitable Zone?

R. Wordsworth^{1,2} ¹ School of Engineering and Applied Sciences, Harvard University, Cambridge, MA 02138, USA² Department of Earth and Planetary Sciences, Harvard University, Cambridge, MA 02138, USA; rwordsworth@seas.harvard.edu

Received 2021 March 19; revised 2021 April 11; accepted 2021 April 14; published 2021 May 4

Abstract

Understanding when global glaciations occur on Earth-like planets is a major challenge in climate evolution research. Most models of how greenhouse gases like CO₂ evolve with time on terrestrial planets are deterministic, but the complex, nonlinear nature of Earth's climate history motivates study of nondeterministic climate models. Here a maximally simple stochastic model of CO₂ evolution and climate on an Earth-like planet with an imperfect CO₂ thermostat is investigated. It is shown that as stellar luminosity is increased in this model, the decrease in the average atmospheric CO₂ concentration renders the climate increasingly unstable, with excursions to a low-temperature state common once the received stellar flux approaches that of present-day Earth. Unless climate feedbacks always force the variance in CO₂ concentration to decline rapidly with received stellar flux, this means that terrestrial planets near the inner edge of the habitable zone may enter Snowball states quite frequently. Observations of the albedos and color variation of terrestrial-type exoplanets should allow this prediction to be tested directly in the future.

Unified Astronomy Thesaurus concepts: [Earth \(planet\) \(439\)](#); [Exoplanets \(498\)](#); [Habitable planets \(695\)](#); [Habitable zone \(696\)](#); [Greenhouse gases \(684\)](#); [Surface ices \(2117\)](#)

Investigating the processes that determine planetary habitability and predicting their observable consequences is a key objective of exoplanet climate modeling (Seager 2013). Today, Earth is still our only confirmed example of a habitable planet, so its climate and chemistry continues to drive our understanding of habitability in general. One of the most influential models of long-term CO₂ evolution on Earth is the carbonate-silicate weathering feedback (Walker et al. 1981), which is the basis for the “canonical” definition of the habitable zone (Kasting et al. 1993; Kopparapu et al. 2013). Despite the popularity of this model, the nature of Earth's CO₂ cycle through geologic time remains a highly active area of research, and a number of processes likely cause Earth's carbon cycle to deviate significantly from the standard weathering feedback (Maher & Chamberlain 2014; Macdonald et al. 2019; Graham & Pierrehumbert 2020).

Accurate estimates of temperature and atmospheric CO₂ in Earth's deep-time history are difficult to obtain, but there is no evidence for secular warming of the climate over the last 4 Gyr (Feulner 2012). Because the Sun's luminosity has increased with time (by about 30%–40% over the last 4 Gyr) and CO₂ has likely been a key greenhouse gas throughout Earth history, a secular decline in atmospheric CO₂ with time seems almost certain. However, this decline has been far from monotonic: current anthropogenic emissions aside, the variations in Earth's surface temperature and atmospheric CO₂ levels just in the last 400 Myr have been substantial, for reasons that are still the subject of intensive study (Franks et al. 2014; Lenardic et al. 2016; Montañez et al. 2016; Macdonald et al. 2019).

Motivated by these observations and previous modeling efforts, the purpose of this note is to construct a simple stochastic model of CO₂ evolution, and to apply it to terrestrial-type planets. The model is intentionally semi-empirical, rather than mechanistic, because many of the processes that affect Earth's CO₂ levels remain so uncertain. As will be shown, the transition to a stochastic view of CO₂ evolution leads to

qualitatively different conclusions compared to the deterministic picture.

Surface temperature evolution in the model is represented as

$$C \frac{dT}{dt} = \frac{1}{4} F [1 - A(T)] - \text{OLR}, \quad (1)$$

where T is surface temperature, C is the heat capacity of the ocean-atmosphere system (here in $\text{J m}^{-2} \text{K}^{-1}$), F is incident stellar flux, and OLR is the outgoing longwave radiation at the top of the atmosphere, which we will take to be a function of T and the molar concentration of CO₂ in the atmosphere. Internal climate variability, which would add a stochastic term to (1), is neglected here to keep the focus on the impact of variability in the CO₂ cycle.

The aim here is to point out general model features rather than to make precise predictions, so we linearize the OLR around Earth's preindustrial surface temperature $T_0 = 288 \text{ K}$ and CO₂ molar concentration $f_{\text{CO}_2,0} = 280 \text{ ppmv}$:

$$\text{OLR} \approx \text{OLR}_0 + a(T - T_0) - b \log(f_{\text{CO}_2}/f_{\text{CO}_2,0}). \quad (2)$$

Here $a = 2 \text{ W m}^{-2} \text{K}^{-1}$ following Abbot (2016), and $b = 5.35 \text{ W m}^{-2}$ is the radiative forcing coefficient for CO₂ (Myhre et al. 1998). Logarithmic dependence of OLR on f_{CO_2} is a reasonable approximation in the $10\text{--}10^5 \text{ ppmv}$ CO₂ and $280\text{--}290 \text{ K}$ temperature range, although the value of b begins to increase at high CO₂ concentrations.

Setting $F = F_0 + \Delta F$ and noting that $\frac{1}{4} F_0 (1 - A_0) = S_0 = \text{OLR}_0$, where $F_0 = 1366 \text{ W m}^{-2}$ and $A_0 = 0.3$ are Earth's present-day received solar flux and albedo, respectively, we can write the time evolution of the temperature deviation from the baseline state $x = T - T_0$ as

$$C \frac{dx}{dt} = \Delta S - \frac{1}{4} F \Delta A - ax + b \log y, \quad (3)$$

where $y = f_{\text{CO}_2}/f_{\text{CO}_2,0}$, $\Delta A = A(T) - A_0$, and $\Delta S = \Delta F(1 - A_0)/4$ (Abbot 2016). ΔA is quite hard to assess in general due to cloud effects, but its dependence on surface ice coverage acts to accelerate Snowball transitions as the transition temperature is approached. As the main aim here is to assess the likelihood of a Snowball transition as a function of atmospheric CO₂ concentration, rather than to study the Snowball state itself, it can be safely set to zero. In addition, the climate achieves thermal balance far more rapidly than atmospheric CO₂ levels change, so we set $dx/dt = 0$. This allows the temperature deviation from the present-day Earth value to be written as

$$x = \frac{\Delta S + b \log y}{a}. \quad (4)$$

Next, we incorporate CO₂ evolution. The evolution of the CO₂ molar concentration y with time is modeled as an Ornstein–Uhlenbeck process with an offset term χ (Jacobs 2010). For a given time step dt , this means that the increment in y is

$$dy = -\tau^{-1}(y - \chi)dt + g dW. \quad (5)$$

Here g is a constant and dW represents a Wiener process such that for every time step dt , dW is equal to a value taken from a Gaussian distribution with variance dt . τ is a timescale that determines how rapidly y is drawn back to the mean value (either by carbonate-silicate weathering feedbacks, or some other process). At each time step, y is set to $-y$ if $y < 0$, ensuring that y always remains positive valued.

Equation (5) provides an inherently nondeterministic representation of CO₂ evolution, with a linear restoration term that prevents unbounded growth in the probability distribution for y with time. From any starting condition, the system evolves toward a statistically steady state on a timescale τ . Once a steady state is reached, the probability density function for y has the form

$$q(y) = Q e^{-(y-\chi)^2/2\sigma_y^2}, \quad (6)$$

where the standard deviation $\sigma_y = \sqrt{\tau/2} g$ and the normalization factor

$$Q = \frac{2}{\sigma_y \sqrt{2\pi}} \frac{1}{1 + \text{erf}[\chi/\sqrt{2}\sigma_y]} \quad (7)$$

ensure

$$\int_0^\infty q(y) dy = 1. \quad (8)$$

Because y can only take positive values, the mean of this distribution is

$$\bar{y} = \int_0^\infty y q(y) dy = \chi + \sigma_y^2 q_0, \quad (9)$$

where $q_0 = q(0)$. The distribution variance is

$$V = \int_0^\infty (y - \bar{y})^2 q(y) dy = \sigma_y^2 (1 - \bar{y} q_0). \quad (10)$$

Note that when $\chi \gg \sigma_y$, $\bar{y} = \chi$ and $V = \sigma_y^2$.

Converting (5) into a statement about the probability of a Snowball transition under given conditions requires the parameter χ to be determined. Given the lack of evidence for secular warming of Earth over the last 4 Gyr as the Sun's

luminosity has increased, the simplest assumption we can make is that CO₂ feedbacks set χ at a value that yields $\bar{T} = T_0$ (and hence $\bar{x} = 0$) on long timescales. Taking the time mean of (3) and assuming separation of timescales between slow (>100 Myr) evolution of ΔS and more rapid stochastic CO₂ fluctuations yields

$$\overline{\log y} = -\Delta S/b = S_0(1 - \alpha)/b, \quad (11)$$

where $\alpha = F/F_0$ is the stellar flux received relative to Earth's present-day received flux. χ is then calculated for use in (5) by finding the root of the function

$$\Phi(\chi) = \overline{\log y} - \int_0^\infty \log y q(y, \chi) dy \quad (12)$$

numerically. Situations where $\Phi(\chi)$ has no root for $\chi > 0$ occur at low χ/σ_y values, but this is of little practical significance here, because the planet enters a Snowball state before they are reached.

Because temperature depends directly on the CO₂ concentration, a second probability density function $p(x)$ for the temperature deviation x can be written as

$$p(x) = q[y(x)] \left| \frac{dy}{dx} \right|. \quad (13)$$

We can rearrange (4) in terms of y , take the derivative, and substitute in the result along with (6) to get

$$p(x) = c Q e^{cx - \Delta S/b - \frac{1}{2}(e^{cx - \Delta S/b} - \chi)^2/\sigma_y^2}, \quad (14)$$

where $c = a/b$. Given (13), we can also write $q(f_{\text{CO}_2}) = q(y)/f_{\text{CO}_2,0}$ and $p(T) = p(x)$. The function $p(x)$ is asymmetric, with rapid decline at high x values but a long tail stretching to low x values (Figure 1). The implication is that for a Gaussian CO₂ concentration distribution with a given variance, very low temperatures are reached more frequently than very high temperatures. Hence, even when the mean CO₂ concentration is well above the threshold for a Snowball event, there remains a finite probability of a transition occurring.

Figure 1 shows the results of solving (5) numerically via the Euler method over 1 Gyr of constant stellar luminosity. CO₂ and temperature time series are shown for a single run (panels (a) and (c)), and probability density functions $q(f_{\text{CO}_2})$ and $p(T)$ are shown for an ensemble of 1024 runs (panels (b) and (d)). The asymmetry of the temperature evolution indicated by (14) is clear from Figure 1(d). In the time series shown, CO₂ levels temporarily dip low enough to make temperature fall below the Snowball threshold (set here at 280 K, following Pierrehumbert et al. 2011) just after 300 Myr. This was verified to cause a Snowball transition when ice-albedo effects were included in the model (results not shown).

Figure 2 shows the output of the same model when secular evolution of stellar flux is included. Here, 3.5 Gyr of evolution is simulated and stellar flux evolution is represented as

$$\alpha(t) = \frac{1}{1 + \frac{2}{5}(1 - t/4.5 \text{ Gyr})}, \quad (15)$$

which is appropriate for a Sun-like star (Gough 1981). Generalization of the results to other star types is straightforward in principle, but it is not pursued here, in part because Snowball transitions on low-mass stars may be strongly affected by the stellar spectrum and the planet's spin-orbit

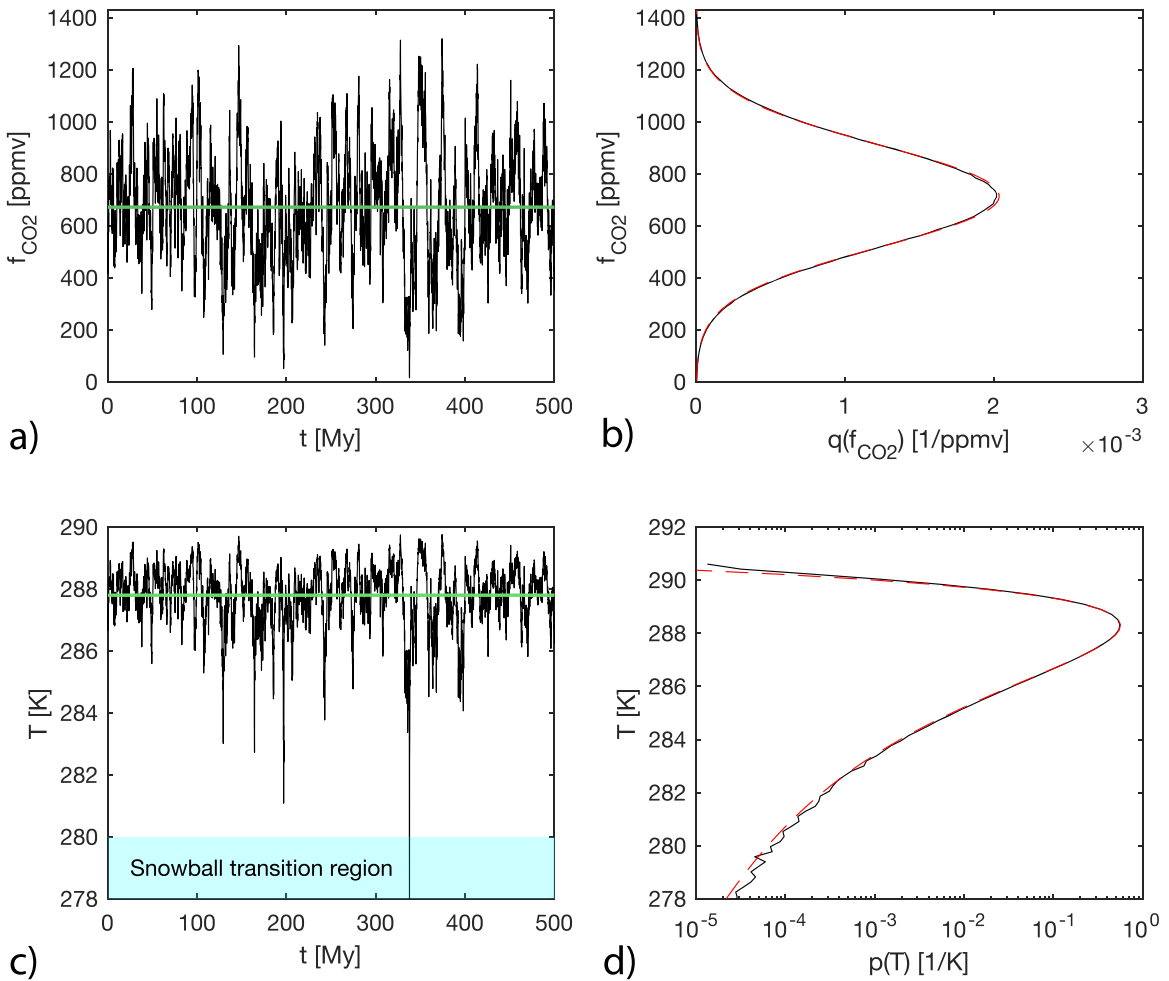


Figure 1. Output of the numerical stochastic model over 500 Myr for an ensemble of 1024 runs, given fixed stellar luminosity ($\alpha = 0.98$), relaxation timescale $\tau = 2.5$ Myr, and $\sigma_y = 0.7$. (a) CO_2 molar concentration vs. time, (b) normalized histogram of CO_2 molar concentration values, (c) temperature vs. time, and (d) normalized histogram of temperature values. For (a) and (c), a single run where temperature dropped below the Snowball limit is shown in black. In (c) the light blue shading indicates the Snowball transition region, while in both (a) and (c), the green line indicates the mean value. Finally, in (b) and (d) the solid black and red dashed lines indicate the numerical results and analytic results according to (6) and (14), respectively. The ice-albedo feedback is not included in these simulations.

configuration (Joshi & Haberle 2012; Shields et al. 2013; Checlair et al. 2017).

As can be seen from Figure 2, for a fixed value of σ_y , temperature fluctuations steadily increase with time until a Snowball transition occurs, with larger σ_y values yielding earlier Snowball transitions. A Snowball event at some point in time is therefore inevitable unless σ_y declines at least as fast as χ does. This result shows that if a planet possess an effective CO_2 thermostat on long timescales (>100 Myr), as Earth appears to, but the shorter-term variance in CO_2 does not decline rapidly as stellar luminosity increases, the chance of undergoing a Snowball glaciation should *increase* as the planet gets closer to the inner edge of the habitable zone. This is a very different prediction from that of deterministic models of CO_2 cycles on Earth-like planets, which either predict permanently clement conditions, or glaciations that only begin to occur toward the outer edge of the habitable zone (e.g., Tajika 2007; Haqq-Misra et al. 2016).

Figure 3 shows the time of Snowball transition for 32 simulations with different values of σ_y . There is some scatter because of the stochastic nature of the simulations, but the strong dependence of transition time on the CO_2 variance is clear. As a general rule, once χ drops to below 2 to 4 times the value of σ_y , a Snowball transition becomes likely. The effect of

τ on the results was also tested, and it was found that a larger τ caused transitions to occur at a given time at slightly higher σ_y/χ ratios in general, although the effect was not large in the $\tau = 0.1$ to 10 Myr range.

Short-term climate variability due to effects like stellar fluctuations, ocean-atmosphere feedbacks, and volcanic aerosol emissions (e.g., Foster & Rahmstorf 2011; Macdonald & Wordsworth 2017; Arnscheidt & Rothman 2020) has been neglected here. Recent work has elegantly demonstrated the impact of short-term climate variability on Snowball transitions in a probabilistic framework (Lucarini & Bódai 2019). Including this variability would simply increase the probability of a Snowball transition for a given set of parameters in Equation (5). Of course, on a planet where stellar, albedo, and dynamical variability always dominates variations in greenhouse gas concentrations, the trend described above would be masked by these effects. However, for Earth at least it is clear that variations in CO_2 concentration have been a fundamental driver of climate change over geologic time.

Reliable constraints on σ_y on Earth on long timescales are hard to come by, although it does appear to have declined over the last Gyr or so since the Neoproterozoic Snowball events. Three-dimensional climate modeling suggests the Marinoan

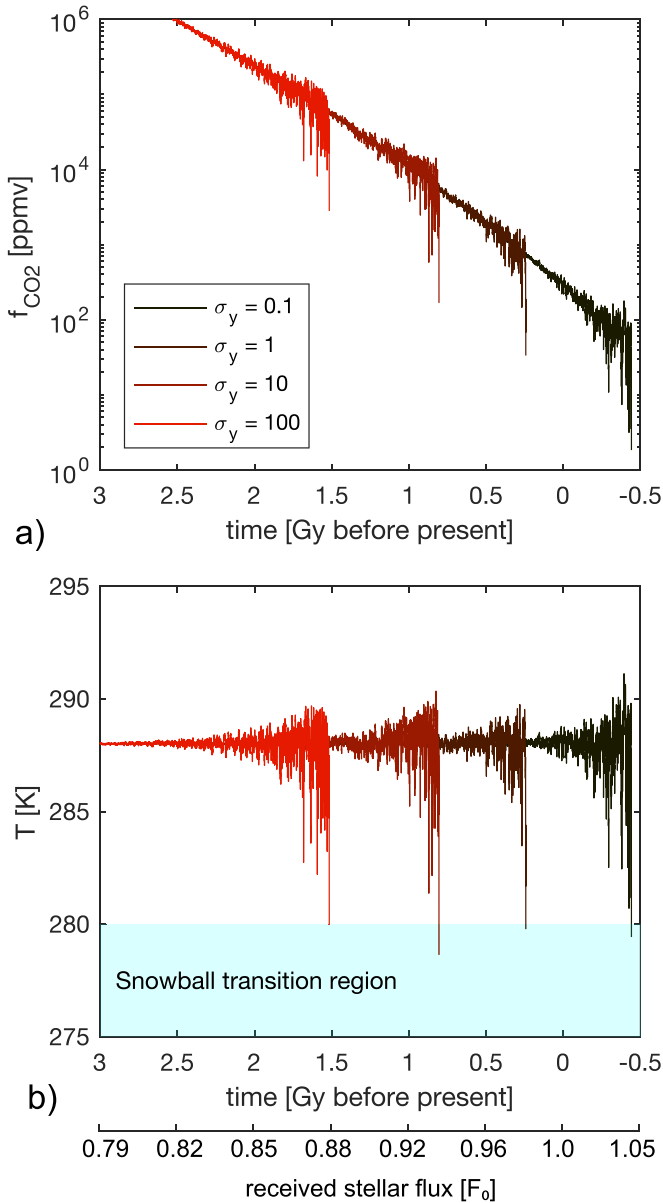


Figure 2. Output of the numerical stochastic model for an Earth-like planet around a G-star with evolving stellar luminosity over 3.5 Gyr, starting from 3 Gyr before present. (a) Atmospheric CO₂ molar concentration and (b) global mean temperature as a function of time. Received stellar flux is also shown on the x-axis. In (b), the light blue shading indicates the Snowball transition region.

Snowball glaciation that terminated 635 Myr ago occurred at a CO₂ concentration of between 280 and 560 ppmv (Voigt et al. 2011; Voigt & Abbot 2012). This can be compared with the 3000 ppmv or more CO₂ that would likely have been present under temperate or warm climate conditions (Pierrehumbert et al. 2011). Over the last 400 Myr, the characteristics of fossil leaf stomata and other proxies constrain CO₂ to around 250–2000 ppmv, with the greatest uncertainty at the highest concentrations (Franks et al. 2014). Finally, over just the last 800 kyr until the industrial era, CO₂ has varied between about 280 and 180 ppmv (Lüthi et al. 2008), with a standard deviation σ_y of 0.11 of the mean value (mean $f_{\text{CO}_2} = 224$ ppmv, $\sigma_f = 25$ ppmv). A few hundred Myr in the future, the stochastic model predicts that CO₂ fluctuations of this order (σ_f of a few

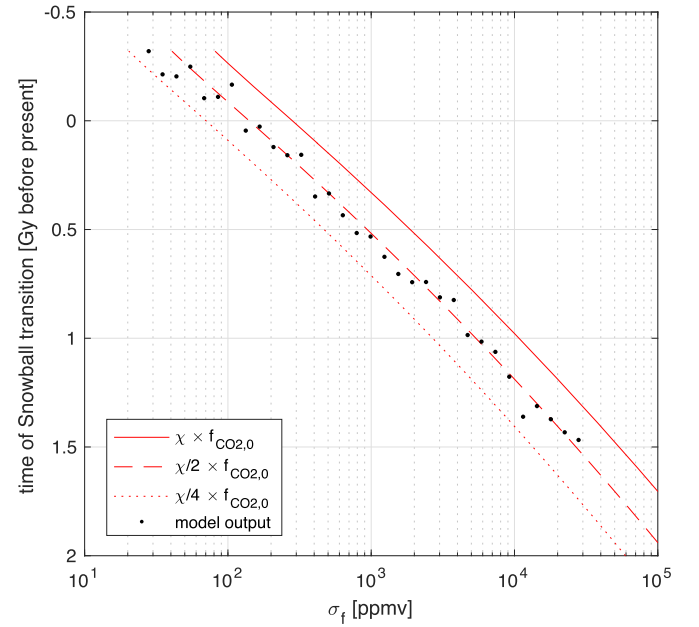


Figure 3. Time of Snowball transition as a function of CO₂ concentration standard deviation σ_f in ppmv ($\sigma_f = \sigma_y \times 280$ ppmv). Black dots show numerical model results, while the red lines show fractions of the steady-state parameter χ , which is calculated from (12).

tens of ppmv) would be sufficient to start a Snowball transition (Figure 3).

The model presented here is extremely simple and empirical. However, it is arguably at least as justified for exoplanet habitability modeling as the many other more sophisticated deterministic models of CO₂ evolution that currently exist. It is of course possible that variance in f_{CO_2} does always decrease rapidly enough as stellar luminosity increases to prevent Snowball transitions. However, even if CO₂ variance has decreased on Earth since the Neoproterozoic, it is not at all obvious based on our current understanding of the carbon cycle that this trend will continue to hold in the future, or apply in general to Earth-like exoplanets.

The long-term CO₂ source in the carbon cycle (volcanism) behaves largely independently of climate until Venus-like atmospheric pressures are reached, with possible modest *positive* feedbacks due to couplings between sea level and the rate of mid-ocean ridge volcanism (Huybers & Langmuir 2017). The CO₂ weathering sink has a temperature dependence, but this can readily become saturated because of local physical weathering rate limits, even when the global climate is temperate. Earth’s history in the Phanerozoic (Maher & Chamberlain 2014; Macdonald et al. 2019) and Neoproterozoic (Hoffman et al. 1998) indicates that the effects of tectonic processes and continental drift on CO₂ variability are both extremely important. Large Igneous Province (LIP) eruptions, which have appeared intermittently throughout Earth’s history, are capable of supplying huge quantities of weatherable basalt to the surface and hence drawing down large quantities of CO₂, even at the cooler equatorial temperatures expected near a Snowball transition. Indeed, weathering associated with LIPs likely played a major role in the first Neoproterozoic Snowball Earth transition (Cox et al. 2016).

The final major source of complexity in Earth’s CO₂ cycle is the biosphere. It is plausible, although certainly not guaranteed, that life itself can rapidly reduce CO₂ variance as stellar

luminosity increases, which would be a clear example of a “Gaian” feedback (Lovelock & Margulis 1974). Surface weathering by land plants is an important part of the modern carbon cycle, and it has been suggested that weathering feedbacks involving C_3 -photosynthetic plants may have buffered minimum f_{CO_2} values to 100–200 ppmv on Earth over the last 24 Myr (Pagani et al. 2009). However, positive biogeochemical ocean feedbacks are a plausible explanation for the ice-age CO_2 oscillations observed over the last 800,000 kyr (Sigman et al. 2010), and coal formation in the Carboniferous may have brought Earth closer to a Snowball than at any time since the Neoproterozoic (Feulner 2017). Even during the last glacial maximum $\sim 20,000$ yr ago, estimates of global mean temperature (Tierney et al. 2020) suggest only a few Kelvins of additional cooling could have been sufficient to push Earth into a Snowball state. As our current era of anthropogenic global warming makes clear, when the starting atmospheric CO_2 inventory is small, even relatively small changes in exchange rates with other reservoirs in the system have the capacity to cause sudden and dramatic shifts in climate.

Tests of the canonical carbonate-silicate weathering hypothesis via observations of atmospheric CO_2 on exoplanets has been proposed (Bean et al. 2017), although they require a large sample size of planetary targets and highly capable observing systems to be successful (Lehmer et al. 2020). Broadband or spectrally resolved albedo measurements to identify planets in a Snowball state provide an alternative approach, at least as long as degeneracies associated with planetary radius and the presence of thick cloud decks can be addressed (Cowan et al. 2011; Guimond & Cowan 2018). Such observations would allow a powerful probe into the level of control that climate feedback mechanisms on terrestrial-type planets provide, and the extent to which Earth’s climate history has been unusual.

This article has benefited from discussions with E. Tziperman and A. Knoll and helpful comments from an anonymous reviewer. Code to reproduce the plots in the paper is available open-source at https://github.com/wordsworthgroup/stochastic_snowball_2021. Finally, I thank R. Pierrehumbert for bringing a manuscript preprint by R. J. Graham (Graham 2021) to my attention during the review process that independently puts forward ideas related to those presented here, although with a different focus and modeling approach.

ORCID iDs

R. Wordsworth  <https://orcid.org/0000-0003-1127-8334>

References

- Abbot, D. S. 2016, *ApJ*, **827**, 117
- Arnscheidt, C. W., & Rothman, D. H. 2020, *RSPSA*, **476**, 20200303
- Bean, J. L., Abbot, D. S., & Kempton, E. M.-R. 2017, *ApJL*, **841**, L24
- Checlair, J., Menou, K., & Abbot, D. S. 2017, *ApJ*, **845**, 132
- Cowan, N. B., Robinson, T., Livengood, T. A., et al. 2011, *ApJ*, **731**, 76
- Cox, G. M., Halverson, G. P., Stevenson, R. K., et al. 2016, *E&PSL*, **446**, 89
- Feulner, G. 2012, *RvGeo*, **50**, RG2006
- Feulner, G. 2017, *PNAS*, **114**, 11333
- Foster, G., & Rahmstorf, S. 2011, *ERL*, **6**, 044022
- Franks, P. J., Royer, D. L., Beerling, D. J., et al. 2014, *GeoRL*, **41**, 4685
- Gough, D. O. 1981, *Physics of Solar Variations* (Berlin: Springer), 21
- Graham, R. J. 2021, arXiv:2104.01224
- Graham, R. J., & Pierrehumbert, R. 2020, *ApJ*, **896**, 115
- Guimond, C. M., & Cowan, N. B. 2018, *AJ*, **155**, 230
- Haqq-Misra, J., Koppapapu, R. K., Batalha, N. E., Harman, C. E., & Kasting, J. F. 2016, *ApJ*, **827**, 120
- Hoffman, P. F., Kaufman, A. J., Halverson, G. P., & Schrag, D. P. 1998, *Sci*, **281**, 1342
- Huybers, P., & Langmuir, C. H. 2017, *E&PSL*, **457**, 238
- Jacobs, K. 2010, *Stochastic Processes for Physicists: Understanding Noisy Systems* (Cambridge: Cambridge Univ. Press)
- Joshi, M. M., & Haberle, R. M. 2012, *AsBio*, **12**, 3
- Kasting, J. F., Whitmire, D. P., & Reynolds, R. T. 1993, *Icar*, **101**, 108
- Koppapapu, R. K., Ramirez, R., Kasting, J. F., et al. 2013, *ApJ*, **765**, 131
- Lehmer, O. R., Catling, D. C., & Krissansen-Totton, J. 2020, *NatCo*, **11**, 1
- Lenardic, A., Jellinek, A. M., Foley, B., O’Neill, C., & Moore, W. B. 2016, *JGRE*, **121**, 1831
- Lovelock, J. E., & Margulis, L. 1974, *Tell*, **26**, 2
- Lucarini, V., & Bódai, T. 2019, *PhRvL*, **122**, 158701
- Lüthi, D., Le Floch, M., Bereiter, B., et al. 2008, *Natur*, **453**, 379
- Macdonald, F. A., Swanson-Hysell, N. L., Park, Y., Lisiecki, L., & Jagoutz, O. 2019, *Sci*, **364**, 181
- Macdonald, F. A., & Wordsworth, R. 2017, *GeoRL*, **44**, 1938
- Maher, K., & Chamberlain, C. P. 2014, *Sci*, **343**, 1502
- Montañez, I. P., McElwain, J. C., Poulsen, C. J., et al. 2016, *NatGe*, **9**, 824
- Myhre, G., Highwood, E. J., Shine, K. P., & Stordal, F. 1998, *GeoRL*, **25**, 2715
- Pagani, M., Caldeira, K., Berner, R., & Beerling, D. J. 2009, *Natur*, **460**, 85
- Pierrehumbert, R. T., Abbot, D. S., Voigt, A., & Koll, D. 2011, *AREPS*, **39**, 417
- Seager, S. 2013, *Sci*, **340**, 577
- Shields, A. L., Meadows, V. S., Bitz, C. M., et al. 2013, *AsBio*, **13**, 715
- Sigman, D. M., Hain, M. P., & Haug, G. H. 2010, *Natur*, **466**, 47
- Tajika, E. 2007, *EP&S*, **59**, 293
- Tierney, J. E., Zhu, J., King, J., et al. 2020, *Natur*, **584**, 569
- Voigt, A., & Abbot, D. S. 2012, *CliPa*, **8**, 2079
- Voigt, A., Abbot, D. S., Pierrehumbert, R. T., & Marotzke, J. 2011, *CliPa*, **7**, 249
- Walker, J. C. G., Hays, P. B., & Kasting, J. F. 1981, *JGR*, **86**, 9776